Aβ-directed Single-chain Antibody Delivery Via a Serotype-1 AAV Vector Improves Learning Behavior and Pathology in Alzheimer's Disease Mice

Deborah A Ryan[1,2], Michael A Mastrangelo[2], Wade C Narrow[2], Mark A Sullivan[3], Howard J Federoff[4] and William J Bowers[2,5,6]

[1]Interdepartmental Graduate Program in Neuroscience, University of Rochester Medical Center, Rochester, New York, USA; [2]Center for Neural Development and Disease, University of Rochester Medical Center, Rochester, New York, USA; [3]Department of Biochemistry asnd Biophysics, University of Rochester Medical Center, Rochester, New York, USA; [4]Department of Neurology, Georgetown University Medical Center, Washington, District of Columbia, USA; [5]Department of Neurology, University of Rochester Medical Center, Rochester, New York, USA; [6]Department of Microbiology and Immunology, University of Rochester Medical Center, Rochester, New York, USA

Alzheimer's disease (AD) is a progressive dementing disorder characterized by age-related amyloid-beta (Aβ) deposition, neurofibrillary tangles, and synapse and neuronal loss. It is widely recognized that Aβ is a principal pathogenic mediator of AD. Our goal was to develop an immunotherapeutic approach, which would specifically lead to the clearance and/or neutralization of Aβ in the triple transgenic mouse model (3xTg-AD). These mice develop the amyloid and tangle pathologies and synaptic dysfunction reminiscent of human AD. Using a human single-chain variable fragment (scFv) antibody phage display library, a novel scFv antibody specific to Aβ was isolated, its activity characterized *in vitro*, and its open reading frame subsequently cloned into a recombinant adeno-associated virus (rAAV) vector. Three-month-old 3xTg-AD mice were intrahippocampally infused with serotype-1 rAAV vectors encoding Aβ-scFv or a control vector using convection-enhanced delivery (CED). Mice receiving rAAV1-Aβ-scFv harbored lower levels of insoluble Aβ and hyperphosphorylated tau, and exhibited improved cognitive function as measured by the Morris Water Maze (MWM) spatial memory task. These results underscore the potential of gene-based passive vaccination for AD, and provide further rationale for the development of Aβ-targeting strategies for this debilitating disease.

Received 1 February 2010; accepted 11 May 2010; published online 15 June 2010. doi:10.1038/mt.2010.111

INTRODUCTION

Amyloid-beta (Aβ) has emerged as a key player in the pathogenesis of Alzheimer's disease (AD),[1] and has been implicated in driving the emergence of other neuropathological manifestations of AD, including neurofibrillary tangles, synaptic dysfunction, and eventual neuronal demise.[2–4] Several groups have approached the challenge of developing a treatment for AD by employing immunotherapeutic strategies designed to specifically target Aβ with promising results.[5,6] A subset of AD patients receiving active vaccinations with fibrillarized $A\beta_{1-42}$ and an adjuvant in a phase II clinical trial unexpectedly developed severe brain inflammation.[7] Significant titers of circulating anti-Aβ antibodies were detected in patients, as well as altered amyloid plaque deposition patterns at autopsy.[8] Follow-up studies have suggested that the observed aseptic meningoencephalitis was caused by infiltrating T-cells or an Fc-mediated response from incitement of an inflammatory T_H1-driven anti-Aβ immune response during vaccination.[7,9]

Safer alternatives to active immunization are being considered, including several which aim to employ passive vaccination with monoclonal antibodies. Full-length antibodies possess an Fc domain, which engages cytotoxic effector functions through complement and mediates binding to the Fc-receptor on phagocytes.[10] This could induce anti-antibody immune responses over time that may diminish therapeutic efficacy or even potentiate inflammatory reactions within the AD brain.[11] Others have demonstrated Aβ clearance can be achieved using antibody fragments that lack the Fc domain.[12–14] We hypothesized that delivery of a recombinant adeno-associated viral (rAAV) vector harboring a gene encoding a single-chain variable fragment (scFv) antibody directed against Aβ would facilitate its clearance, mitigate downstream pathological cascades, and lead to improved cognitive function. scFvs are composed of a variable heavy and variable light chain connected by a linker, which is expressed as a single polypeptide. The flexible 14-amino acid linker permits the variable heavy and variable light chains freedom to align in the correct antigen binding orientation.[15,16]

rAAV vector-mediated delivery of *scFv* genes has distinct advantages over chronic/intermittent infusion of full-length antibodies, including long-term gene expression, low immunogenicity, and wide brain parenchymal distribution. Additional benefits, including

Correspondence: *William J Bowers, Department of Neurology, Center for Neural Development and Disease, University of Rochester Medical Center, 601 Elmwood Avenue, Box 645, Rochester, New York, USA. E-mail: william_bowers@urmc.rochester.edu*

lack of an Fc region, relate to the small size of scFvs (~30 kd), which enhances tissue penetration. Other investigators have applied rAAV technology for the delivery of *scFv* genes to target Aβ.[17–19] Although they have reported significant clearance of Aβ and lack of vector-associated toxicity, our present study addresses two unanswered issues relating to the effects of chronic anti-Aβ scFv expression on tau pathology and learning and memory behavior.

Using a human scFv phage display library, we isolated a novel scFv antibody specific to Aβ, which was characterized *in vitro* and its gene subsequently packaged into a rAAV vector. Triple

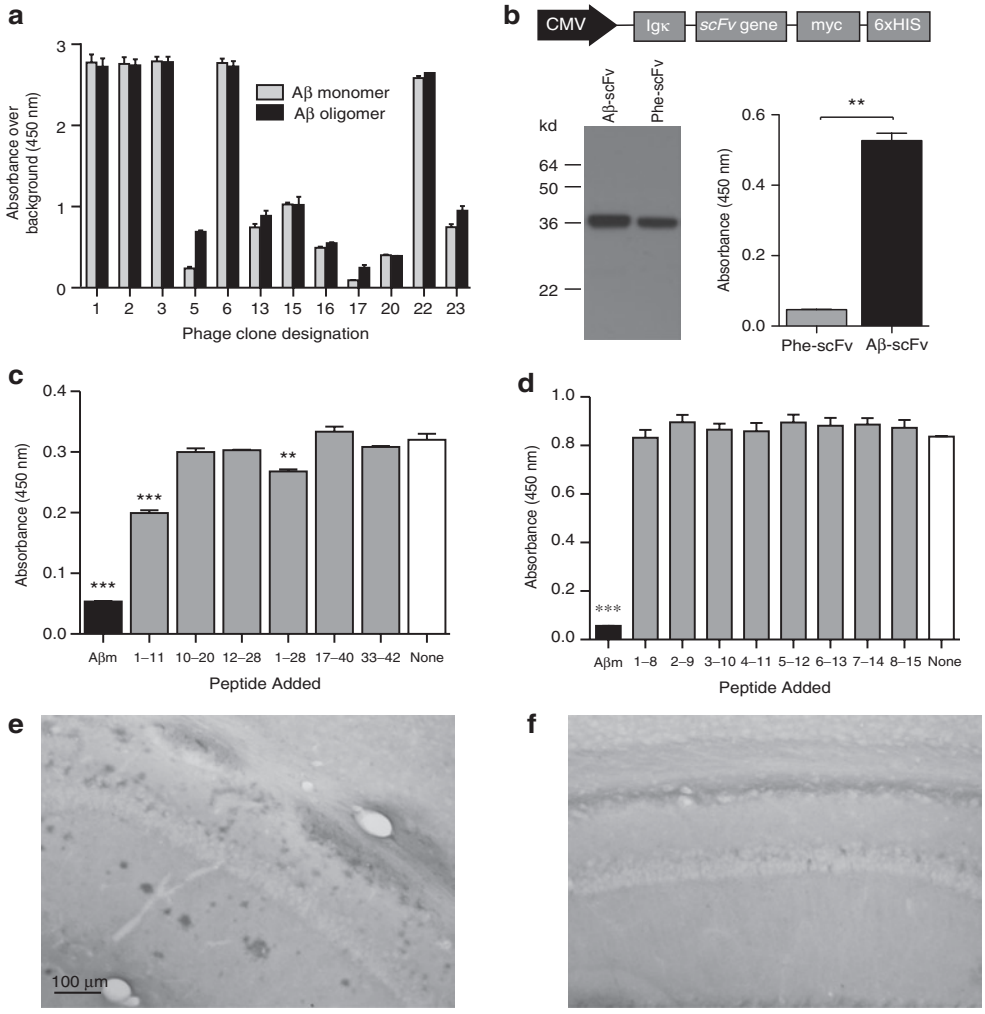

Figure 1 Isolation and characterization of an Aβ-specific scFv antibody from a human scFv phage display library. Aβ antigen was used to coat 96-well plates and the phage library was added. Aβ-binding clones were isolated and successively panned and enriched over a total of three rounds. (**a**) The resultant phage clones were tested by phage ELISA to determine whether their displayed scFvs were specific to Aβ monomer, Aβ oligomer, or both. Clone #2, recognizing both monomer and oligomer, was chosen for subsequent studies and named "Aβ-sFv." The *scFv* gene was subcloned into a mammalian expression vector pSecTag2 (Invitrogen). (**b**) Mammalian expression testing of scFv clones. A schematic representation of the pSecTag2-scFv construct is shown to illustrate the CMV promoter (black) and the open reading frame elements (gray), including the murine Ig κ-chain secretion signal, the scFv sequence (either Aβ-scFv or Phe-scFv, a nonrelevant control) and the carboxy-terminal c-myc epitope and hexahistidine tags. The pSecTag2-scFv plasmids were transiently transfected into BHK cells. Culture media (CM) was harvested 48 hours following transfection and analyzed via SDS-PAGE and ELISA. The myc epitope tags, on the c-terminus of the scFv, were detected by western blot using an HRP-conjugated anti-myc antibody (Invitrogen). Ninety-six well plates were coated with Aβ peptide and the harvested CM was subsequently added to the well. Unbound proteins were washed away and the anti-myc-HRP antibody was then used to detect the scFv that remained bound to the well. An unpaired *t*-test was performed to determine significant differences ($P = 0.0019$). (**c**,**d**) Aβ-scFv epitope mapping. Full-length Aβ monomer was coated onto plastic wells, Aβ-scFv (produced in mammalian cells) was preincubated with equimolar concentrations of various Aβ peptide fragments before being added to these wells. After incubating for 2 hours, unbound Aβ-scFv was washed from the wells and an anti-myc HRP conjugated antibody was used to detect the presence of bound Aβ-scFv. Low absorbance indicates that a peptide fragment bound to Aβ-scFv thereby blocking its interaction with the Aβ monomer-coated well. High absorbance indicated that Aβ-scFv was not specific for the peptide competitor fragment. Large peptide fragments were used initially (**c**) to narrow down a region of interest, followed by overlapping octa-peptides from amino acids 1–8 through 8–15. A one-way ANOVA was performed (**c**) $P < 0.0001$; (**d**) $P < 0.0001$ with a Bonferroni's post-test to compare all columns to the no-peptide negative control (**$P < 0.01$; ***$P < 0.001$). (**e**) Aβ-scFv- and (**f**) Phe-scFv-containing culture media was used to stain brain tissue from 24-month-old 3xTg-AD mice and an anti-myc HRP antibody was used for detection with DAB development. The CA1 region of the hippocampus is shown. 3xTg, triple transgenic; AD, Alzheimer's disease; ANOVA, analysis of variance; Aβ, amyloid-beta; BHK, baby hamster kidney; CMV, cytomegalovirus; ELISA, enzyme-linked immunosorbent assay; HRP, horseradish peroxidase; scFv, single-chain variable fragment; SDS-PAGE, sodium dodecyl sulfate-polyacrylamide gel electrophoresis.

transgenic (3xTg-AD) mice, which develop age-related amyloid and tau pathologies and early cognitive deficits,[20,21] received bilateral hippocampal stereotactic infusions using convection-enhanced delivery (CED).[22] Treatment of 3-month-old 3xTg-AD mice resulted in decreased amyloid burden, decreased tau hyperphosphorylation, and improved spatial learning by 12 months of age.

RESULTS

Isolation and *in vitro* characterization of an Aβ-specific scFv antibody

Isolation of an scFv specific to Aβ was accomplished by exploiting a phage display library expressing scFvs of human immunoglobulin.[23] The display of human scFv antibodies on the phage surface occurs via fusion to the phage M13 pIII minor coat protein (**Supplementary Figure S1**). Selection of the library was performed on a synthetic Aβ peptide preparation, which included monomer as well as low- and high-order oligomers. The general binding specificity of the resultant phage clones was assessed by phage enzyme-linked immunosorbent assay (ELISA) (**Figure 1a**). Of the 24 clones chosen, 19 were reactive to some form of Aβ above background levels, 12 of which harbored unique coding sequences. From sequence analysis clones #1 and 2 were most abundant each present four and nine times, respectively. Clone #2, which recognized monomer and oligomer equally well, was chosen for subsequent study and named "Aβ-scFv." Genes for Aβ-scFv and Phe-scFv, a nonrelevant control scFv antibody that recognizes the hapten Phenobarbital,[24] were subcloned into the mammalian expression vector, pSecTag2 (Invitrogen, Carlsbad, CA) (**Figure 1b**). Transient transfection of pSecTag2-scFv plasmids into baby hamster kidney cells yielded culture media (CM)-containing scFv protein for characterization. Western analysis demonstrated both Phe-scFv and Aβ-scFv protein bands at the expected molecular weight (~30 kd; **Figure 1b**). Aβ-scFv maintained its original binding specificity after expression from mammalian cells as demonstrated by scFv ELISA. Aβ-scFv bound Aβ protein significantly greater than Phe-scFv (**Figure 1b**). Aβ-scFv epitope mapping was performed to further elucidate its binding characteristics (**Figure 1c,d**). To determine the cognate epitope recognized by Aβ-scFv, large peptide fragments were initially employed (**Figure 1c**). Peptide fragments within the N-terminus of Aβ were able to partially compete with $Aβ_{1–42}$ monomer for Aβ-scFv. $Aβ_{1–11}$ and $Aβ_{1–28}$ were found to significantly, but incompletely, block binding when compared to the no-peptide control, whereas full-length $Aβ_{1–42}$ completely blocked binding. Eight overlapping N-terminal octa-peptides were tested to compete for Aβ-scFv binding to full-length Aβ-coated wells, given the partial inhibition of binding by $Aβ_{1–11}$ and $Aβ_{1–28}$ (**Figure 1d**). None of the octa-peptides blocked binding of Aβ-scFv to $Aβ_{1–42}$ monomer-coated wells, suggesting Aβ-scFv recognizes a conformational or discontinuous epitope of $Aβ_{1–42}$ that includes amino acids at the N-terminus. Aβ-scFv (**Figure 1e**) and Phe-scFv-containing CM (**Figure 1f**) was used to stain tissue from 24-month-old 3xTg-AD mice. Aβ-scFv stained cell-associated Aβ, as well as extracellular plaques throughout areas of the cortex, hippocampus, subiculum and entorhinal cortex, whereas Phe-scFv did not exhibit specific staining.

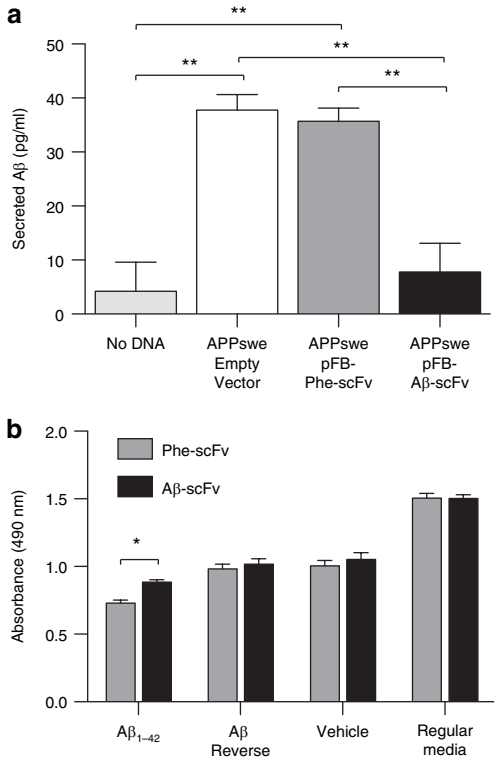

Figure 2 Aβ-scFv antibody reduces detection of secreted Aβ and mitigates Aβ-mediated toxicity *in vitro*. (**a**) Neuro2a cells were cotransfected with a human APP Swedish mutation (*APPswe*) transgene and a plasmid containing the gene for Aβ-scFv, Phe-scFv, or an empty vector. Aβ, secreted from the transfected cells into the culture media, was measured by ELISA (Covance BetaMark x-42 kit, Covance). Cells undergoing transfection conditions without DNA served as a control to establish background levels for the assay. A one-way ANOVA was performed ($P = 0.0007$) with Bonferroni's post-test (**$P < 0.01$). (**b**) Primary cortical neurons were treated on day *in vitro* 8 with 5 µmol/l synthetic $Aβ_{1–42}$ peptide, $Aβ_{42–1}$ reverse peptide, or vehicle only. The Aβ peptides aggregated under conditions which induced an array of species including monomer, low- and high-order oligomers, and trace amounts of insoluble aggregates. CM-containing Phe-scFv and Aβ-scFv was purified using HisPur cobalt spin columns (Pierce). The purified scFv proteins were incubated with the $Aβ_{1–42}$ peptide, $Aβ_{42–1}$ reverse peptide, vehicle, or regular media for 1 hour before addition to the cortical neurons. Forty-eight hours following treatment cell viability was assessed using an MTS reduction assay (Promega, Madison, WI) and absorbance measure at 490 nm. A two-way ANOVA was used to determine differences in treatment ($P < 0.0001$), scFv type ($P < 0.05$) and interaction between those variables ($P = 0.1471$) with a Bonferroni's post-test (*$P < 0.05$). ANOVA, analysis of variance; Aβ, amyloid-beta; APPswe, amyloid precursor protein Swedish mutation; CM, culture media; ELISA, enzyme-linked immunosorbent assay; scFv, single-chain variable fragment.

Aβ-scFv binds Aβ and prevents toxicity *in vitro*

We next sought to determine whether expression of Aβ-scFv by a neuronal cell line could disrupt Aβ secretion/detection *in vitro* (**Figure 2a**). Neuro2a cells, a neuronal immortalized cell line, were cotransfected with an amyloid precursor protein (APP) Swedish mutation (*APPswe*) transgene-expressing plasmid and a plasmid containing the gene for Aβ-scFv, Phe-scFv or an empty vector; levels of secreted Aβ were subsequently measured. Cells transfected with *APPswe*/empty vector and *APPswe/Phe-scFv* secreted similar concentrations of $Aβ_{1–42}$ into the CM, which were

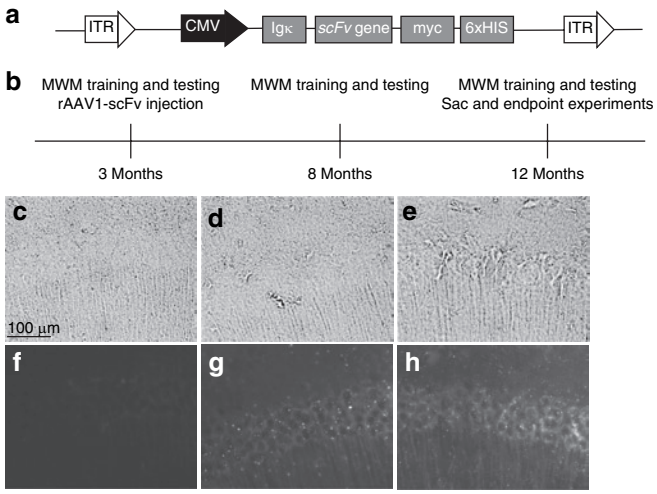

Figure 3 Experimental design and *in vivo* Aβ-scFv expression from AAV1 constructs. (**a**) A schematic representation of the rAAV expression cassette. Inverted terminal repeat (ITR) sequences flank the CMV promoter (black) and the open reading frame elements (gray). The open reading frame consists of the murine Ig κ-chain secretion signal, the scFv sequence (either *Aβ-scFv* or *Phe-scFv*) and the carboxy-terminal c-myc epitope and hexahistidine tags. rAAV-scFv constructs were packaged into serotype-1 rAAV capsids. (**b**) Experimental timeline: 3xTg-AD mice were trained on the MWM at 3 months of age. If predetermined criteria of learning and memory performance were met, a mouse was included in the study. Mice meeting criteria were separated into one of three groups: no treatment, Phe-scFv, or Aβ-scFv. Animals in the no-treatment group did not receive an injection. Mice received bilateral CED hippocampal injections of rAAV1 capsids. MWM training and testing was performed again at 8 and 12 months of age. At each age mice were required to learn a new platform location. After the final MWM session mice were sacrificed and their brains collected for biochemical and pathological analysis. (**c–h**) *In vivo* expression of scFv protein. 3xTg-AD mice injected at 3 months were sacrificed at 12 months and brains processed for immunohistochemical analysis of scFv expression using an anti-myc antibody (9B11) and Alexa 488 fluorescent secondary for detection. (**c–e**) Bright field images and (**f–h**) fluorescent images were acquired for (**c**,**f**) noninjected control, (**d**,**g**) rAAV1-Phe-scFv, and (**e**,**h**) rAAV1-Aβ-scFv mice. CA1 region of the hippocampus is shown. Bar = 100 μm. 3xTg, triple transgenic; AAV1, adeno-associated virus type 1; AD, Alzheimer's disease; Aβ, amyloid-beta; CED, convection-enhanced delivery; CMV, cytomegalovirus; MWM, Morris Water Maze; rAAV, recombinant AAV; scFv, single-chain variable fragment.

significantly higher than what was detected from cells cotransfected with *APPswe/Aβ-scFv*. Aβ-scFv is blocking secretion of Aβ and/or binding secreted Aβ and preventing its detection by obscuring its epitope. These results suggest that neuronal Aβ-scFv expression can effectively interact with Aβ in a cell culture context, but does not speak to whether Aβ-scFv blocks Aβ-induced neurotoxicity. We subsequently incubated $A\beta_{1-42}$ with purified Aβ-scFv, Phe-scFv, or media, and added these samples to primary mouse cortical neurons. An MTS-based viability assay demonstrated that neurons incubated with Aβ peptide and Phe-scFv exhibited significantly lower viability than neurons treated with Aβ peptide and Aβ-scFv (**Figure 2b**).

In vivo Aβ-scFv delivery to 3xTg-AD mice via a serotype-1 AAV vector

Aβ-scFv and *Phe-scFv* were subcloned into recombinant adeno-associated viral (rAAV) vectors (**Figure 3a**), packaged into serotype-1 particles, and tested by HEK293A transduction and western blot to confirm expression (data not shown). AAV serotype-1 capsids are neurotropic and demonstrate increased transduction efficiencies and enhanced parenchymal spread as compared to the more commonly utilized serotype-2.[25] Three-month-old 3xTg-AD mice, which develop age-related amyloid and tau pathologies reminiscent of human AD, were initially trained in the Morris Water Maze (MWM) behavioral paradigm and were required to meet performance criteria before their further inclusion in the study (**Figure 3b**). Mice meeting performance criteria were randomized into treatment groups and received stereotactic bilateral hippocampal injections of rAAV1-Aβ-scFv or rAAV1-Phe-scFv employing CED.[22] Each mouse was trained and tested again on the MWM at 8 and 12 months of age. Twelve-month-old mice were sacrificed and their brains collected for immunohistochemical (IHC) and biochemical analyses. IHC analysis of *in vivo* scFv expression was performed using an anti-myc antibody. Mice receiving no injection (**Figure 3c,f**) showed only background levels of myc epitope staining. 3xTg-AD mice receiving rAAV1-Phe-scFv (**Figure 3d,g**) and rAAV1-Aβ-scFv (**Figure 3e,h**) harbored staining in and around cell bodies of the hippocampus, expanding both rostrally and caudally from the injection site. In a few mice scFv expression appeared to extend just anterior to the hippocampus with extremely low levels of scFv protein detected in tissue surrounding the ventricular space (data not shown), however, scFv expression in the majority of animals was isolated to the hippocampus.

Impact of rAAV1 Aβ-scFv on learning and memory

The MWM is a behavioral test wherein the location of a hidden platform must be learned and remembered. At 3, 8, and 12 months of age, each mouse was required to learn a new platform location. Latency to reach the platform was used as a measure of performance (**Figure 4a–c**). Mice at 3 and 8 months of age did not exhibit any differences between treatment groups (3 months, $P = 0.2809$; 8 months, $P = 0.3118$), but did demonstrate their ability to learn over the 5 days of training (3 and 8 months, $P < 0.0001$). Latencies of 12-month-old mice (**Figure 4c**) treated with rAAV1-Aβ-scFv were shorter than mice treated with rAAV1-Phe-scFv ($P = 0.0535$), with significant differences in means at day 2 (post-test, $P < 0.05$). Both treatment groups at 12 months were still able to learn over the course of 5 days ($P < 0.0001$), but these data demonstrate 3xTg-AD mice infused with rAAV encoded Aβ-scFv learned the new platform location more quickly. Probe trials consisted of a 30-second swim where the platform had been removed from the pool. Probe trials served two purposes: to control for the possibility that mice could "sense" the platform location and to test short and long-term memory. Two probe trials were administered 1.5 and 24 hours after the final training trial on the fifth day (**Figure 4d,e**). One measure to assess probe trial performance is the amount of time spent in the goal quadrant. By the fifth day of training, both rAAV1-Phe-scFv- and rAAV1-Aβ-scFv-treated mice had learned the platform location equally well and there were no differences between groups on probe trial measures. Cumulative index is a measure that assesses how much a subject deviates from an ideal path to the goal (**Figure 4f**). Lower cumulative indexes denote a more direct path was taken. rAAV1-Aβ-scFv-treated mice exhibited lower

cumulative indexes at 12 months than rAAV1-Phe-scFv-treated mice ($P = 0.0273$), with significant differences in means at day 2 (post-test $P < 0.05$). A survival analysis to analyze the earliest day a mouse met criteria was performed (**Figure 4g**). Mice that failed to reach criteria during the study were marked at 5 days, however, those values were censored, thus weighted differently than data from mice that actually met criteria by day 5. The curves from the two treatment groups were compared demonstrating a higher percentage of mice receiving rAAV1-Aβ-scFv reached criteria earlier. During training the number of trials that each mouse either "hit goal" or "timed-out" was tabulated. At 12 months of age, the number of trials that mice "timed out" was greater for 3xTg-AD mice receiving rAAV1-Phe-scFv than rAAV1-Aβ-scFv injected counterparts (**Figure 4h**).

Pathological assessment of Aβ-scFv in the 3xTg-AD mouse

To determine the effect of rAAV1-Aβ-scFv on Aβ burden, ELISAs for soluble and insoluble $A\beta_{40}$ and $A\beta_{42}$ were performed on homogenates prepared from microdissected hippocampi (**Figure 5a,b** and **Supplementary Table S1**). There was no difference in the ratio of total soluble $A\beta_{42/40}$ between treatment and control groups. The ratio of insoluble $A\beta_{42/40}$ was significantly decreased in mice receiving rAAV1-Aβ-scFv compared to rAAV1-Phe-scFv (**Figure 5b**). Although there was no reduction of total soluble Aβ, levels of soluble oligomeric Aβ, as measured via NU-4 dot blot, were reduced in mice treated with rAAV1-Aβ-scFv as compared to mice receiving no injection (**Figure 5c**). Mice receiving rAAV1-Phe-scFv possessed an intermediate level of soluble oligomeric Aβ. To further assess the status of insoluble Aβ, Congo red, a classic histological stain for amyloid-fibrils, was employed. A characteristic yellow–green bifringence is observed upon visualizing Congo red-stained amyloid plaques under polarized light (**Figure 5d–f**). Mice treated with rAAV1-Aβ-scFv exhibited >75% reduction in numbers of Congo red-stained plaques (**Figure 5g**). Examination of microglia by IHC using ionized calcium-binding adaptor molecule-1 (IBA-1) antibody demonstrated an increase in IBA-1 immunopositive pixels in mice receiving rAAV1-Aβ-scFv over mice given no injection (**Figure 6d**). Again rAAV1-Phe-scFv-treated animals showed an intermediate level of IBA-1 immunopositive pixels. To assess what this difference in immunopositive pixels represented, the numbers of microglia were determined. There was a small, but significant increase in numbers of nonresting microglia in mice receiving rAAV1-Aβ-scFv as compared to rAAV1-Phe-scFv and no-treatment mice (**Figure 6e**). Numbers of activated microglia were greater in rAAV1-Aβ-scFv treated mice over noninjected controls; rAAV1-Phe-scFv mice exhibited an intermediate number (**Figure 6f**). IHC analysis using 6E10 antibody, which recognizes

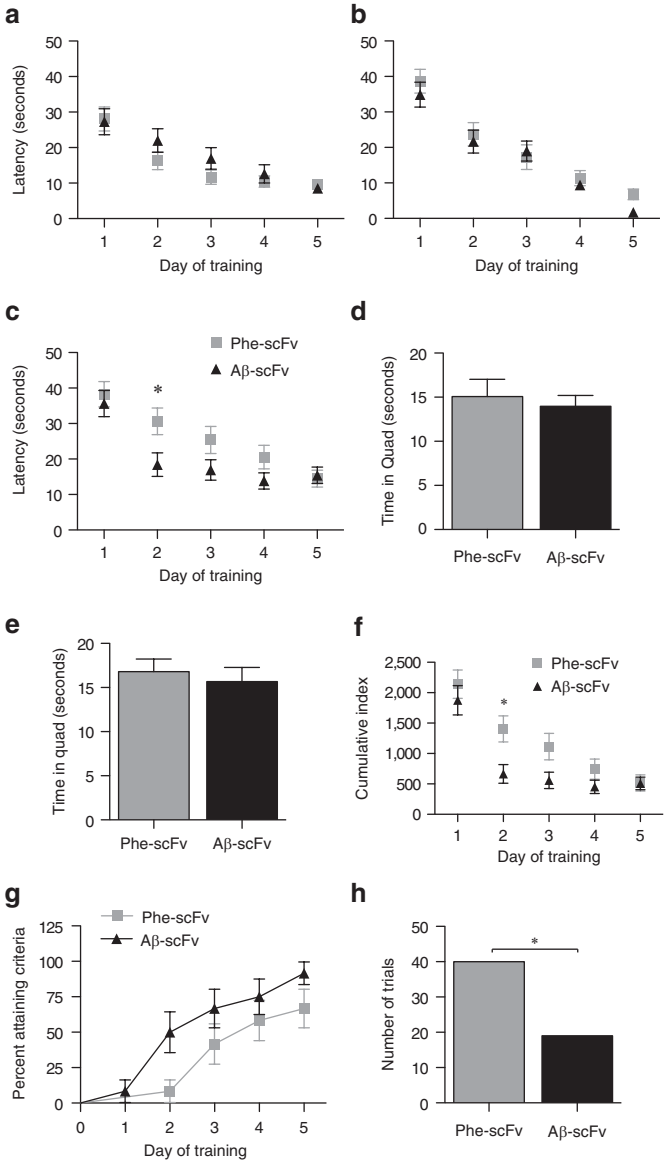

Figure 4 3xTg-AD mice receiving AAV1 Aβ-scFv learn a new target location sooner than those receiving AAV1 Phe-scFv during training on the Morris Water Maze (MWM). Three-month-old 3xTg-AD mice received bilateral, hippocampal injections of rAAV1-Phe-scFv or rAAV1-Aβ-scFv. Mice were trained and tested on the MWM at (**a**) 3, (**b**) 8, and (**c**) 12 months of age. At each time point mice were required to learn a new hidden platform location over 5 days of training. The amount of time to reach the hidden platform, or latency, was used as a measure of performance. Repeated measures ANOVA with Bonferroni post-test were used to analyze the data. Probe trials were conducted (**d**) 1.5 and (**e**) 24 hours after the final training trial and to assess short and long-term memory, respectively. The hidden platform was removed during the probed trials and mice are allowed to free swim for 30 seconds. The amount of time spent in the goal quadrant was used as a measure of performance; an unpaired *t*-test compared the two means (**d**) $P = 0.6354$; (**e**) $P = 0.6005$. (**f**) Cumulative index was employed as a measure of performance that assesses whether a subject deviates from an ideal path to the goal. The lower the index, the closer an individual followed an ideal path. Repeated measures ANOVA with Bonferroni post-test were used to analyze the data. (**g**) An established measure of performance criteria was the requirement that a given mouse reach the platform in 15 seconds, or less, on average over three trials in 1 day. A survival analysis was performed where the event was defined as the earliest day to reach criteria. The percent of mice reaching criteria per day in each group is shown. A Gehan–Breslow–Wilcoxon test was used to compare the curves from the two treatment groups (**g**) $P = 0.0529$. (**h**) During the training trials, mice were given 60 seconds to locate the hidden platform. The mouse could either "hit goal" or the trial was "timed out" if the platform was not located. After a "timed-out" trial, the experimenter physically guided the mouse to the platform. A Fisher's exact test was used to determine a significant difference for this contingency between treatment groups (**h**) $P = 0.0041$. 3xTg, triple transgenic; AAV1, adeno-associated virus type 1; AD, Alzheimer's disease; ANOVA, analysis of variance; Aβ, amyloid-beta; rAAV, recombinant AAV.

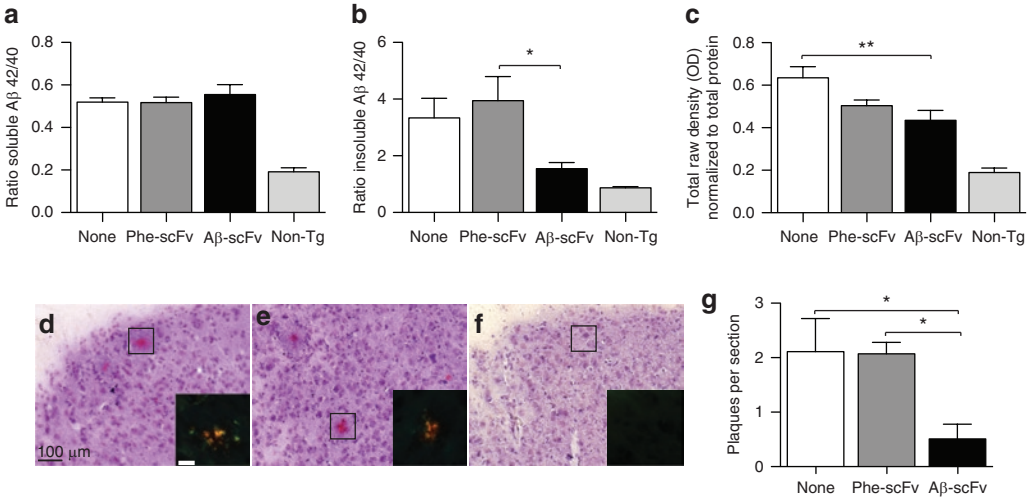

Figure 5 AAV1 vector-mediated expression of Aβ-scFv antibody decreases levels of insoluble Aβ in the hippocampus of 3xTg-AD mice. Three-month-old 3xTg-AD mice received bilateral, hippocampal injections of rAAV1-Phe-scFv, rAAV1-Aβ-scFv, or no injection. The mice were sacrificed at 12 months of age and half of each brain was microdissected for the generation of protein homogenates and the other half processed for preparation of histological sections. ELISAs for soluble and insoluble $A\beta_{40}$ and $A\beta_{42}$ were performed on hippocampal protein and levels were expressed as a ratio of $A\beta_{42}$:$A\beta_{40}$. The ratio of soluble (**a**) $A\beta_{42/40}$ and (**b**) insoluble $A\beta_{42/40}$ are shown. (**c**) Hippocampal protein homogenates were absorbed on nitrocellulose and blotted with an oligomer-specific antibody, NU-4, and β-actin. Densitometry was performed and NU-4 levels of immunoreactivity were normalized to β-actin. Histological sections from mice receiving (**d**) no treatment, (**e**) rAAV1-Phe-scFv, or (**f**) rAAV1-Aβ-scFv injections were stained with Congo red and counterstained with hematoxylin. (**g**) Congo red-positive plaques were enumerated from regions within the hippocampus; images shown (**d**–**f**) were taken within the subiculum. (**d**) Bar = 100 µm; inset bar in **d** is 200 µm. Nontransgenic animals were not included in statistical analyses, but were used to demonstrate baseline levels of staining. One-way ANOVA with Bonferroni's multiple comparisons post-tests were performed between treatment and control columns. One-way ANOVA (**a**) $P = 0.6684$, (**b**) $P = 0.0286$, (**c**) $P = 0.0093$, and (**g**) $P = 0.0319$. A capped line with an asterisk was used to indicate when two groups had statistically different means as determined by the post-test (*$P < 0.05$; **$P < 0.01$). 3xTg, triple transgenic; AAV1, adeno-associated virus type 1; AD, Alzheimer's disease; ANOVA, analysis of variance; Aβ, amyloid-beta; ELISA, enzyme-linked immunosorbent assay; rAAV, recombinant AAV; scFv, single-chain variable fragment.

both human Aβ and APP, revealed marked differences in the number of 6E10 immunopositive pixels in the CA1 of scFv-injected 3xTg-AD mice (**Figure 7a,c,e,g,i**). Mice receiving rAAV1-Phe-scFv or no injection showed elevated Aβ/APP staining as compared to mice receiving rAAV1-Aβ-scFv (**Figure 7i**). Nontransgenic CA1 images are shown to demonstrate background levels where no human Aβ or APP is expressed (**Figure 7g**). Hyperphosphorylated tau is a pathological hallmark in human AD. IHC analysis using an antihyperphosphorylated tau antibody (AT180) demonstrated that nontreated and rAAV1-Phe-scFv-treated mice have significant levels of hyperphosphorylated tau (**Figure 7b,d,j**). Interestingly, mice receiving rAAV1-Aβ-scFv have greatly diminished staining for hyperphosphorylated tau (**Figure 7f,j**). Nontransgenic animals show background levels of staining (**Figure 7h**).

DISCUSSION

Our results demonstrate that sustained hippocampal expression of an Aβ-specific scFv decreased amyloid burden, diminished hyperphosphorylation of tau, increased numbers of microglia, and enhanced learning behavior. Other investigators have previously reported the use of rAAV-based delivery of Aβ-specific scFvs to mouse models of AD.[17,19,26] Similar to our findings, decreased levels of Aβ and an absence of treatment related toxicity has been reported.[17,19] Moreover, we have recently demonstrated that an $A\beta_{42}$-specific scFv intrabody targeted to the endoplasmic reticulum resulted in decreased extracellular Aβ burden and decreased hyperphosphorylated tau pathology.[26] Although these previous studies speak primarily to the efficacy of scFv-based therapeutics to reduce pathological burden, they have not systematically addressed whether these improvements translate to functional benefit. This study is the first to assess the effects of this therapeutic strategy on learning and memory behaviors following intrahippocampal rAAV-Aβ-scFv delivery in a complex model of the disease.

The 3xTg-AD mouse exhibits age-related accumulation of intraneuronal Aβ, extracellular Aβ, and hyperphosphorylated tau pathologies, as well as synaptic deficits.[20] In addition, young 3xTg-AD mice exhibit cognitive impairments, specifically, a deficit in memory retention on the MWM beginning at 4 months of age.[21] Our study compared the performance of 3xTg-AD mice receiving rAAV1-Aβ-scFv versus rAAV1-Phe-scFv on the MWM at 3, 8, and 12 months of age. We predicted 3-month-old mice would perform without significant impairment, but as the mice age, we would observe a progressive diminution in performance beginning with retention deficits. When analyzing behavioral data trial by trial we did not observe any retention deficits at 8 or 12 months of age. The reason for this could relate to slight differences in behavioral paradigms or maze difficulty. At 3 and 8 months of age there were no differences between treatment groups; on average, both groups learned the platform location at the same rate. At 12 months of age, a difference in the rate of learning emerged between the two treatment groups, where mice receiving rAAV1-Aβ-scFv correctly located the hidden platform by the second day of training, whereas rAAV1-Phe-scFv treated mice gradually learned platform location over the 5 days of training. In a study of the PDAPP (human platelet-defined growth factor β chain promoter-driven amyloid precursor protein

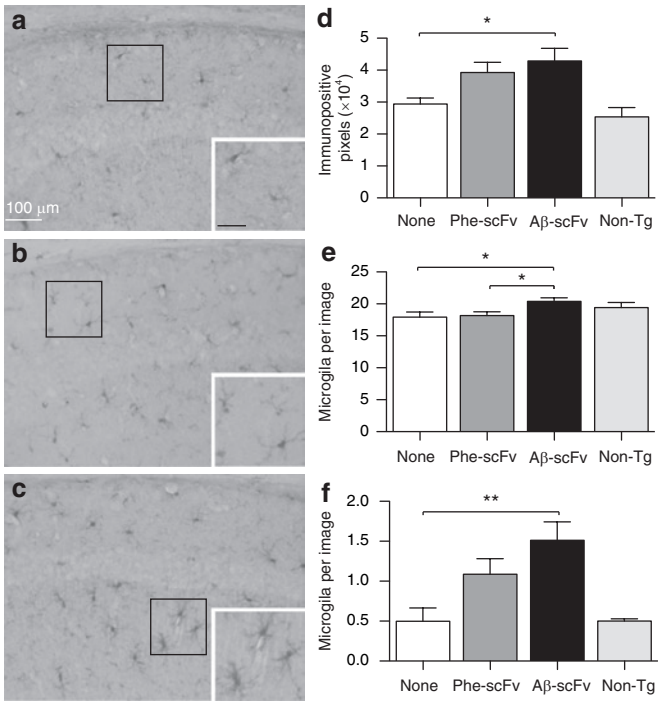

Figure 6 AAV1 vector-mediated expression of the Aβ-scFv antibody increases number and activation of microglia. (**a**) Three-month-old 3xTg-AD mice received no injection, or (**b**) bilateral hippocampal injections of rAAV1-Phe-scFv or (**c**) rAAV1-Aβ-scFv. Mice were sacrificed at 12 months of age and processed for immunohistochemical analyses for IBA-1, which stains microglia. Nontransgenic animals were not included in statistical analyses, but used to demonstrate baseline levels of staining. Representative images are shown. (**a**) Bar =100 μm. Images were taken of the CA1 region of the hippocampus at ×20 magnification and numbers of (**d**) immunopositive pixels, (**e**) nonresting microglia, and (**f**) activated microglia were quantified. One-way ANOVA with Bonferroni's multiple comparisons post-tests were performed between treatment and control columns. One-way ANOVA (**d**) $P = 0.0234$; (**e**) $P = 0.0186$; (**f**) $P = 0.0066$. A capped line with an asterisk was used to indicate when two groups had statistically different means as determined by the post-test (*$P < 0.05$; **$P < 0.01$). 3xTg, triple transgenic; AAV1, adeno-associated virus type 1; AD, Alzheimer's disease; ANOVA, analysis of variance; Aβ, amyloid-beta; rAAV, recombinant AAV; scFv, single-chain variable fragment.

minigene) mouse model, which develops only amyloid pathology, mice exhibited age-related deficits in learning new target locations on the MWM; these deficits were associated with increased plaque deposition.[27] Interestingly, we were able to demonstrate faster learning of platform location in the treatment group exhibiting a decrease in insoluble Aβ levels as measured by ELISA, as well as a marked decrease in numbers of congophilic plaques. Along with changes in Aβ, the diminished levels of hyperphosphorylated tau could also contribute to improved learning in the rAAV1-Aβ-scFv cohort. A tau transgenic mouse model of AD, THY-Tau22, which develops hyperphosphorylated tau and paired-helical filaments, exhibits delayed learning of a novel target platform location in the MWM paradigm.[28] It is important to note that our therapeutic was delivered and spread throughout the hippocampi, but areas of cortex, which also develop pathology, were not treated. Although the hippocampus plays an important role in learning and memory, the cerebral cortex is intimately involved in the execution of these cognitively demanding tasks.

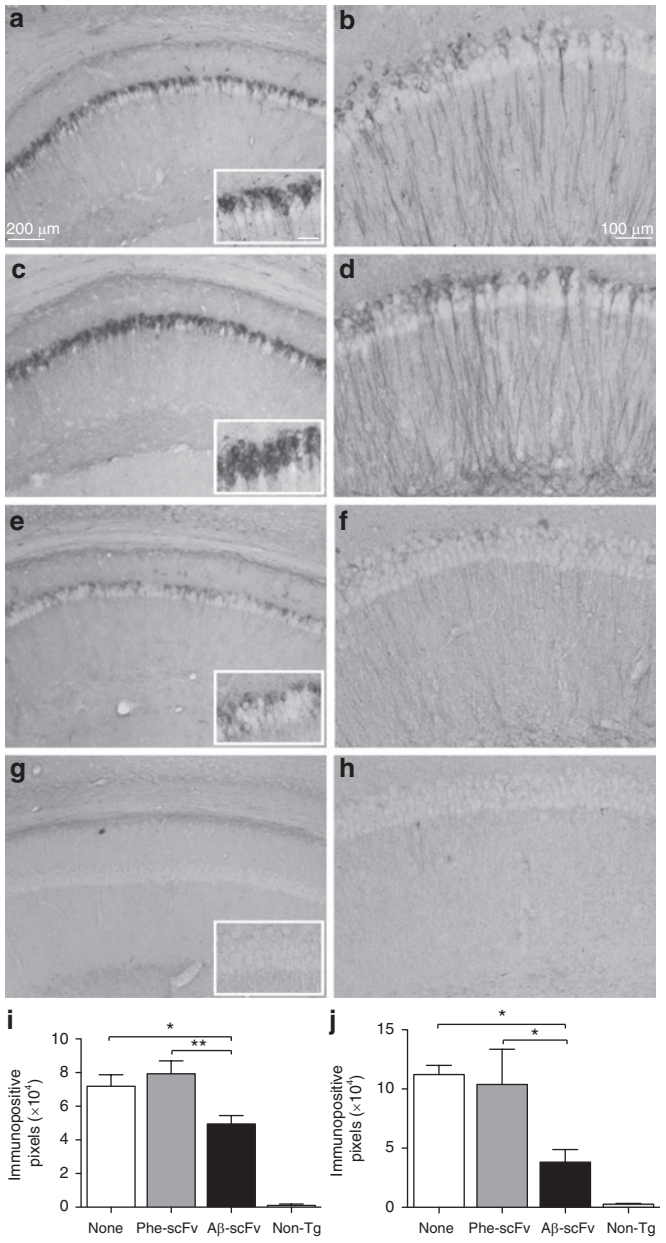

Figure 7 AAV1 vector-mediated expression of the Aβ-scFv antibody decreases levels of Aβ and hyperphosphorylated tau in the hippocampus of 3xTg-AD mice. Three-month-old 3xTg-AD mice received (**a**,**b**) no injection or (**c**,**d**) bilateral, hippocampal injections of rAAV1-Phe-scFv or (**e**,**f**) rAAV1-Aβ-scFv. Mice were sacrificed at 12 months of age and processed for immunohistochemical analyses for Aβ/APP (6E10 antibody; **a**,**c**,**e**,**g**,**i**) and hyperphosphorylated tau (AT180 antibody; **b**,**d**,**f**,**h**,**j**). (**g**,**h**) Nontransgenic animals were not included in statistical analyses, but were used to demonstrate baseline levels of staining. Representative images are shown. (**a**) Bar = 200 μm, while that shown in the inset represents 50 μm; (**b**) Bar = 100 μm. Images were taken of the CA1 region of the hippocampus at ×20 magnification and (**i**,**j**) numbers of immunopositive pixels, per a standard area were quantified. One-way ANOVA with Bonferroni's multiple comparisons post-tests were performed between treatment and control columns. One-way ANOVA (**i**) $P = 0.0061$; (**j**) $P = 0.0198$. A capped line with an asterisk was used to indicate when two groups had statistically different means as determined by the post-test (*$P < 0.05$; **$P < 0.01$). 3xTg, triple transgenic; AAV1, adeno-associated virus type 1; AD, Alzheimer's disease; ANOVA, analysis of variance; APP, amyloid precursor protein; Aβ, amyloid-beta; rAAV, recombinant AAV; scFv, single-chain variable fragment.

An unresolved question relates to the therapeutic mechanism by which scFvs act *in vivo*. Our data suggest several nonmutually exclusive mechanisms may be at play: (i) Aβ-scFv inhibits Aβ release from neurons transduced with the serotype-1 rAAV vector particles. We showed that significantly less Aβ is detected in the CM of neuronally derived cells cotransfected with a human *APPswe* transgene-expressing plasmid and a plasmid containing the gene for *Aβ-scFv* than cells cotransfected with the control plasmid harboring *Phe-scFv*. In this scenario, Aβ could be retained by the scFv in the vesicular lumen and degraded before release. However, an alternate interpretation of these data is that Aβ is bound by Aβ-scFv, thereby preventing its detection. (ii) Aβ-scFv mediates clearance of extracellular Aβ from the brain by an Fc-independent mechanism. Levites and colleagues revealed evidence of scFv-Aβ complexes in the blood plasma of scFv-treated amyloidogenic mice, which represents one means by which extracellularly bound scFv/Aβ complexes could exit the brain. (iii) Aβ-scFv inhibits oligomerization of extraneuronal Aβ. The levels of insoluble Aβ42, oligomeric Aβ by NU-4 and numbers of congophillic plaques were significantly reduced in 3xTg-AD mice receiving rAAV1-Aβ-scFv, suggesting that this third option could at least partially account for the effects observed on amyloid pathology.

Microglia colocalize with amyloid deposits in the human AD brain.[29–31] Consequently, many investigators have studied whether microglia play a role in Aβ deposition or reduction. In a recent report, investigators experimentally ablated brain microglia in APP/PS1 mice using a Herpes simplex virus thymidine kinase/ganciclovir-based strategy.[32] Surprisingly, the absence of microglia did not reduce or enhance plaque deposition without an additional intervention. Bacskai and colleagues used *in vivo* multiphoton fluorescence microscopy to image clearance of Aβ deposits in APP transgenic mice. Whole antibody treatment and application of F(ab′)2 fragments cleared Aβ deposits with enhanced activation of proximal microglia.[33] These findings indicate that Fc-dependent phagocytosis and Fc-independent mechanisms can disrupt Aβ plaque formation.[13] Importantly, an Fc-independent mechanism of microglia phagocytosis of Aβ has been reported, where Aβ was found associated with a cell surface receptor complex of the scavenger receptor CD36, $\alpha_6\beta_1$ integrin, and CD47.[34] An experiment that would selectively inhibit microglial activation during rAAV1-Aβ-scFv treatment would demonstrate the degree to which microglia participate in pathology clearance.

In the present study, we observed a significant increase in IBA-1 immunopositive pixels, numbers of nonresting, and numbers of activated microglia within hippocampi of mice treated with rAAV1-Aβ-scFv compared to noninjected control mice. Mice treated with rAAV1-Aβ-scFv compared to rAAV1-Phe-scFv controls displayed a significant increase in numbers of nonresting microglia, but only a trending increase in levels of IBA-1 immunopositive pixels and numbers of activated microglia. rAAV1-Phe-scFv treated mice exhibited levels of IBA-1 immunopositive pixels and numbers of activated microglia that were at intermediate levels between noninjected and rAAV1-Aβ-scFv. This finding suggests that one or more components of the AAV injection may be acting nonspecifically to incite a minor enhancement in microglia activation, which could be beneficial or detrimental. However, the trending increases are not significantly different from the other treatment cohorts, thus making it difficult to draw definitive conclusions.

Paired with the data demonstrating improved learning in rAAV1-Aβ-scFv-treated mice, these increases in activated microglia could indicate that these cells are directly aiding in clearance of extracellular scFv-Aβ complexes. However, another possibility exists. Streit proposes that accumulating Aβ and hyperphophorylated tau induce dystrophic changes and eventual senescence in the microglial population. Evidence for this phenomenon exists in studies of human AD brains where dystrophic alterations of microglia have been described.[35,36] Hence, the Aβ-scFv mediated decrease in insoluble Aβ that we observe in 3xTg-AD mice are consistent with prevention of senescence of resident microglia, thereby enhancing the abilities of these cells to participate in Aβ clearance. Our results indicate that further study of the mechanism(s) underlying therapeutic benefit of gene-based scFv delivery and the testing of Aβ-scFv in the setting of established AD pathology are warranted.

MATERIALS AND METHODS

Phage scFv clone selection on Aβ oligomer preparations. Construction of the pAP-III_6 human scFv antibody library in a M13 phage display format has been previously described.[23] Fifty microliter per well of Aβ oligomer preparations (11 µmol/l) were coated onto Nunc Maxisorp 96-well plates overnight at 4 °C. The peptide was removed and wells washed with Tris-buffered saline (TBS), blocked for 1 hour with TBS+0.5% casein and aliquots of phage library added. A 50 µl aliquot containing 2–5 × 10^{11} transducing units was added to each well and incubated at room temperature for 2 hours. Wells were washed with TBS+0.5% Tween-20, followed by TBS alone, and then phage was eluted for 15 minutes with 50 µl 0.1 mol/l glycine HCl, pH 2.2. The eluate was collected, neutralized with Tris base, transduced into TG1 *Escherichia coli* and grown overnight on Lysogeny broth. Plates were scraped and colonies evenly suspended, grown to mid-log phase, infected with helper virus and phage isolated to be used for a subsequent round of enrichment. Three rounds of selection and enrichment were performed.

Baby hamster kidney transfection with pSecTag2-scFv constructs. The plasmids were transiently transfected into baby hamster kidney cells. After 48 hours, CM was collected, centrifuged at 16,000*g* for 10 minutes at 4 °C and run on sodium dodecyl sulfate-polyacrylamide gel electrophoresis. ScFv bands were detected by western blot with anti-myc horseradish peroxidase antibody (Invitrogen).

Aβ-scFv epitope mapping. Full-length Aβ monomer was used to coat wells of a 96-well plate overnight at 4 °C. Wells were washed 1× with TBS, and blocked with TBS+0.1% Tween-20 (TBST) casein for 1 hour at room temperature. Aβ-scFv-containing CM was preincubated with equimolar concentrations of various Aβ peptide fragments, full-length monomer, or no peptide for 1 hour before being added to these wells. After incubating for 2 hours, unbound Aβ-scFv was washed from the wells and an anti-myc horseradish peroxidase (Invitrogen) conjugated antibody was used to detect the presence of bound Aβ-scFv. Large peptide fragments were purchased from American Peptide (Sunnyvale, CA). Octa-peptides were ordered from CPC Scientific (San Jose, CA).

Aβ secretion ELISA. Neuro2a cells were cotransfected with a human *APPswe* transgene-expressing plasmid and a plasmid containing the gene for Aβ-scFv, Phe-scFv, or an empty vector. Transfection was accomplished following the protocol for the Nucleofector kit (Lonza, Walkersville, MD). Aβ, secreted from the transfected cells into the CM, was measured by

ELISA (Covance BetaMark x-42 kit; Covance, Berkeley, CA). Cells undergoing transfection conditions without DNA served as a control to establish background levels for the assay.

Cortical neuron viability assay. Primary cortical neurons were treated on day *in vitro* 8 with 5 µmol/l synthetic $A\beta_{1-42}$ peptide, $A\beta_{42-1}$ reverse peptide, or vehicle only. All treatment conditions were prepared identically. The peptides or vehicle were aggregated under Aβ oligomer preparation conditions, and then concentrated 3× via Speed-Vac. The Aβ preps were composed of an array of species including monomer, low- and high-order oligomers, and trace amounts of insoluble aggregates. CM-containing Phe-scFv and Aβ-scFv was purified using HisPur cobalt spin columns (Pierce, Rockford, IL). The purified scFv proteins were incubated with the $A\beta_{1-42}$ peptide, $A\beta_{42-1}$ reverse peptide, vehicle, or regular media for 1 hour before addition to the cortical neurons. Forty-eight hours following treatment cell viability was measured with an MTS reduction assay, where MTS (3-(4,5-dimethylthiazol-2-yl)-5-(3-carboxymethoxyphenyl)-2-(4-sulfophenyl)-2H-tetrazolium), when added to phenazine methosulfate, produces a water-soluble formazan product. Absorbance at 490 nm was used to quantify the relative numbers of live cells between treatment conditions.

Transgenic mice. All animal housing and procedures were performed in compliance with guidelines established by the University Committee of Animal Resources at the University of Rochester. The 3xTg-AD (B1 line) and nontransgenic mice were generously provided by Frank LaFerla (University of California, Irvine[20]). Homozygous male 3xTg-AD and age-matched nontransgenic mice were used in these studies.

Stereotactic injections of rAAV-scFvs via CED. Three month-old 3xTg-AD male mice received bilateral hippocampal stereotactic injections of rAAV1-scFv capsids in accordance with approved University of Rochester animal use guidelines. Under Avertin anesthesia (300 mg/kg), mice were positioned in a stereotactic apparatus and an incision was made to expose bregma on the skull. Two burr holes were drilled bilaterally over the injection coordinates (−2.06 mm bregma, 1.5 mm lateral, −1.25 mm ventral). The injection set up consisted of a frame-mounted micromanipulator, holding an UltraMicro pump (WPI Instruments, Sarasota, FL) with a Hamilton syringe and a 33 GA needle (Hamilton, Reno, NV). The needle was lowered into the parenchyma at a rate of 0.8 mm/minute, and then held in place for 2 minutes before injection. rAAV vectors (1×10^9) transducing units were delivered to each hippocampus in a 5 µl volume. rAAV-scFv capsids were delivered by CED (a method to augment the distribution of molecules delivered into the brain by sustaining a pressure gradient for the duration of the injection) by using increasing step-wise injection rates of 100 nl/minute for 6 minutes, 200 nl/minute for 10 minutes, and 400 nl/minute for 6 minutes. After injection, the needle was allowed to rest in place for 2 minutes, then withdrawn at a rate of 0.4 mm/minute. Incisions were sutured, antibiotic and lidocaine topical ointments were applied, and mice placed in a recovery chamber. At 12 months of age, mice were sacrificed and their brains were perfused with heparinized saline. Half of each brain was microdissected for the generation of protein homogenates and the other half was postfixed in 4% paraformaldehyde and processed for histochemical analyses.

MWM test for spatial learning and memory. The MWM is a behavior test for spatial learning and memory. The maze consists of a pool filled with opaque water, an escape platform, whose surface is just below the water level, and a camera mounted above the pool to track mouse movement. Mice use visual cues in the environment to localize the hidden platform. The pool and platform dimensions are as follows: pool diameter 134 cm, platform 8.8 cm × 8.8 cm, the platform was ~1–2 cm beneath the water surface, the center of the platform is 26.55 cm from the pool wall. Three, 60-second trials were performed per day for 5 days of training. If a mouse did not reach the platform before 60 seconds had expired, the trial was designated "timed-out" and the experimenter would physically guide the mouse to the platform. When a mouse reached the platform it was allowed to rest for 5 seconds before being rescued by the experimenter and returned to its home cage under a warming lamp. Over 5 days of training, the platform location was kept constant for a given mouse, yet the start site varied from trial to trial. Probe trials were conducted 1.5 and 24 hours after the final training trial to assess short and long-term memory, respectively. The hidden platform was removed during the probe trials and mice were allowed to free swim for 30 seconds. Three cued trails were performed on the 6th day when all hidden platform trials and probe trials were completed. In cued trials a flag is placed atop the platform so that mice can see its location. Cued trials are used to control for any visual impairments or motor deficits that would hamper maze performance. At 3 months of age, each mouse was required to meet predetermined performance criteria of reaching the platform in 15 seconds, or less, on average over three trials in 1 day. If a mouse did not meet the criteria within 5 days of training, it was excluded from the study. Mice meeting performance criteria were randomized into treatment groups. Mice were trained and tested on the MWM at 3, 8, and 12 months of age. At each age, mice were required to learn a new hidden platform location over 5 days of training.

Aβ soluble and insoluble ELISAs. Hippocampal homogenates were assayed for levels of soluble and insoluble $A\beta_{40}$ and $A\beta_{42}$ using the Colorimetric x-40 and x-42 BetaMark ELISA kits (Covance). Manufacture's instructions were followed, except a separate standard curve was run for insoluble and soluble standards. Standards were resuspended in the same solution as diluted samples. Insoluble Aβ samples were diluted 1:300 in phosphate-buffered saline (PBS) and soluble Aβ samples diluted 1:5 for x-42 and 1:10 for x-40 in PBS. $N = 10–12$ mice per group.

Soluble Aβ oligomer dot blot. Nitrocellulose membranes were incubated in transfer buffer for 10 minutes, hippocampal homogenates were spotted onto membranes while vacuum pressure was applied. Each dot consisted of 21 µg of total protein. Membranes were dried, blocked for 1 hour at room temperature in TBST and 5% nonfat dried milk. Membranes were subsequently blotted using primary antibody NU-4, an oligomer-specific antibody[37] (provided by Dr William Klein, Northwestern University), at 1:1,000 dilution overnight at 4 °C and washed 4 × 5 minutes with TBST. A horseradish peroxidase-conjugated secondary antibody was used at a 1:2,000 dilution for 1 hour at room temperature, washed as above, then washed 1 × 5 minutes in TBS. The membrane was stripped and reprobed with anti-β-actin (1:5,000) to normalize dots for total protein. Dot blots were visualized with chemiluminescence, and analyzed for total raw density (Labworks by UVP, Upland, CA).

3,3′-Diaminobenzidine immunohistochemistry. Brains postfixed in 4% paraformaldehyde were coronally sectioned on a freezing-stage microtome to 30-µm thick sections. Tissue sections were stored in cryoprotectant at −20 °C until needed. Sections were processed for IHC as previously described[38] using the following antibodies at the given dilutions: microglia—IBA-1, 1:750 (Wako, Richmond, VA); Aβ/APP—6E10, 1:1,000 (Covance); hyperphosphorylated tau—AT180, 1:500 (Pierce). An IHC using CM-containing Aβ-scFv or Phe-scFv was also performed to detect Aβ in 24-month-old 3xTg-AD mice, CM—1:2 dilution, anti-myc horseradish peroxidase secondary, 1:1,000 (Invitrogen). Images of the CA1 region of hippocampus were acquired at ×20 magnification the number of immunopositive pixels above a preset threshold was quantified using MCID 6.0 Imaging Software (Interfocus Imaging, Cambridge, UK). The mean of the number of pixels per standard unit area was taken. Microglia were counted as nonresting if the cell body was hypertrophied and ramified processes retracted, cells were counted as activated if cell body was hypertrophied and thick, short processes were present.

Congo red. Tissue was sectioned and stored as for IHC. Congo red stain was prepared per manufacturer's protocol (Sigma-Aldrich, St Louis, MO). Tissue was stained with Modified Lillie–Meyer's hematoxylin (20% hematoxylin, diluted in dH_2O) for 2.5 minutes, washed with tap water 1 × 30 seconds and 1 × 4 minutes, then placed in Congo red stain for 35 minutes, washed with PBS, and mounted onto glass slides. Tissue was allowed to dry fully on the slides before dipping in 30% ethanol for 30 seconds, dipped in histoclear for 15 seconds, then cover-slipped with mounting media. Images were acquired at ×20 magnification of the hippocampus and the total number of congophilic plaques were counted in each image. The total plaque number was divided by the number of images counted.

Fluorescent immunohistochemistry for scFv detection. Brains postfixed in 4% paraformaldehyde were coronally sectioned on a freezing-stage microtome to 30-μm thick sections. Tissue sections were stored in cryoprotectant at −20 °C until needed. Cryoprotectant was washed off in PBS; sections were permeabilized for 5 minutes with PBS+0.2% Triton X-100, and blocked for 1 hour in PBS+0.1% Triton X-100, 10% normal goat serum (NGS). Primary antibody anti-myc, 9B11 (Cell Signaling, Danvers, MA) was diluted 1:1,000 in PBS+0.1% Triton X-100, 1% NGS, incubated overnight at 4 °C, and sections washed 3 × 10 minutes in PBS+0.1% Triton X-100, 1% NGS. Alexa 488-conjugated secondary antibody (Molecular Probes, Carlsbad, CA) was diluted 1:500 in PBS+0.1% Triton X-100, 1% NGS, incubated for 1 hour, and sections washed 3 × 10 minutes in PBS+0.1% Triton X-100, 1% NGS, then 2 × 5 minutes PBS. Sections were mounted and cover slipped with Mowiol. Images were acquired at ×40 magnification with equal exposure times. Brightness and contrast were adjusted equally on all images.

Statistical analyses. Statistical analysis was performed using GraphPad Prism 5 software (La Jolla, CA). The statistical tests employed are specified in figure legends or results section. Statistical differences with P values of ≤0.05 were considered significant.

Supplementary Materials and Methods include Aβ peptide preparation, phage ELISA, phage clone sequencing, mammalian vector cloning, primary cortical neuron culturing, AAV vector construction and packaging, *in vitro* transduction, and hippocampal homogenate preparation.

SUPPLEMENTARY MATERIAL

Figure S1. A schematic diagram of phage selection for an Aβ-specific scFv antibody.

Table S1. AAV1 vector-mediated expression of Aβ-scFv antibody decreases levels of insoluble $A\beta_{42}$ in the hippocampus of 3xTg-AD mice.

Materials and Methods.

ACKNOWLEDGMENTS

The authors thank William Klein (Northwestern University) for providing the NU-4 antibody, Rita Giuliano (University of Rochester Medical Center) for guidance on culturing mouse primary neurons, and Abbie Stokes-Riner (University of Rochester Medical Center) for advice on statistical analyzes. This work was supported by NIH F31-NS059283 to D.A.R., and NIH R01-AG023593 and NIH R21-AG031878 to W.J.B. The authors declared no conflict of interest.

REFERENCES

1. Scheuner, D, Eckman, C, Jensen, M, Song, X, Citron, M, Suzuki, N *et al.* (1996). Secreted amyloid β-protein similar to that in the senile plaques of Alzheimer's disease is increased *in vivo* by the presenilin 1 and 2 and APP mutations linked to familial Alzheimer's disease. *Nat Med* **2**: 864–870.
2. Lewis, J, Dickson, DW, Lin, WL, Chisholm, L, Corral, A, Jones, G *et al.* (2001). Enhanced neurofibrillary degeneration in transgenic mice expressing mutant tau and APP. *Science* **293**: 1487–1491.
3. Götz, J, Chen, F, van Dorpe, J and Nitsch, RM (2001). Formation of neurofibrillary tangles in P301l tau transgenic mice induced by Aβ 42 fibrils. *Science* **293**: 1491–1495.
4. Oddo, S, Billings, L, Kesslak, JP, Cribbs, DH and LaFerla, FM (2004). Aβ immunotherapy leads to clearance of early, but not late, hyperphosphorylated tau aggregates via the proteasome. *Neuron* **43**: 321–332.
5. Schenk, D, Barbour, R, Dunn, W, Gordon, G, Grajeda, H, Guido, T *et al.* (1999). Immunization with amyloid-β attenuates Alzheimer-disease-like pathology in the PDAPP mouse. *Nature* **400**: 173–177.
6. Bard, F, Cannon, C, Barbour, R, Burke, RL, Games, D, Grajeda, H *et al.* (2000). Peripherally administered antibodies against amyloid β-peptide enter the central nervous system and reduce pathology in a mouse model of Alzheimer disease. *Nat Med* **6**: 916–919.
7. Orgogozo, JM, Gilman, S, Dartigues, JF, Laurent, B, Puel, M, Kirby, LC *et al.* (2003). Subacute meningoencephalitis in a subset of patients with AD after Aβ42 immunization. *Neurology* **61**: 46–54.
8. Hock, C, Konietzko, U, Streffer, JR, Tracy, J, Signorell, A, Müller-Tillmanns, B *et al.* (2003). Antibodies against β-amyloid slow cognitive decline in Alzheimer's disease. *Neuron* **38**: 547–554.
9. Nicoll, JA, Wilkinson, D, Holmes, C, Steart, P, Markham, H and Weller, RO (2003). Neuropathology of human Alzheimer disease after immunization with amyloid-β peptide: a case report. *Nat Med* **9**: 448–452.
10. Raghavan, M and Bjorkman, PJ (1996). Fc receptors and their interactions with immunoglobulins. *Annu Rev Cell Dev Biol* **12**: 181–220.
11. Kuus-Reichel, K, Grauer, LS, Karavodin, LM, Knott, C, Krusemeier, M and Kay, NE (1994). Will immunogenicity limit the use, efficacy, and future development of therapeutic monoclonal antibodies? *Clin Diagn Lab Immunol* **1**: 365–372.
12. Matsuoka, Y, Saito, M, LaFrancois, J, Saito, M, Gaynor, K, Olm, V *et al.* (2003). Novel therapeutic approach for the treatment of Alzheimer's disease by peripheral administration of agents with an affinity to β-amyloid. *J Neurosci* **23**: 29–33.
13. Bacskai, BJ, Kajdasz, ST, McLellan, ME, Games, D, Seubert, P, Schenk, D *et al.* (2002). Non-Fc-mediated mechanisms are involved in clearance of amyloid-β *in vivo* by immunotherapy. *J Neurosci* **22**: 7873–7878.
14. Tamura, Y, Hamajima, K, Matsui, K, Yanoma, S, Narita, M, Tajima, N *et al.* (2005). The F(ab)'2 fragment of an Aβ -specific monoclonal antibody reduces Aβ deposits in the brain. *Neurobiol Dis* **20**: 541–549.
15. Kortt, AA, Malby, RL, Caldwell, JB, Gruen, LC, Ivancic, N, Lawrence, MC *et al.* (1994). Recombinant anti-sialidase single-chain variable fragment antibody. Characterization, formation of dimer and higher-molecular-mass multimers and the solution of the crystal structure of the single-chain variable fragment/sialidase complex. *Eur J Biochem* **221**: 151–157.
16. Zdanov, A, Li, Y, Bundle, DR, Deng, SJ, MacKenzie, CR, Narang, SA *et al.* (1994). Structure of a single-chain antibody variable domain (Fv) fragment complexed with a carbohydrate antigen at 1.7-A resolution. *Proc Natl Acad Sci USA* **91**: 6423–6427.
17. Fukuchi, K, Tahara, K, Kim, HD, Maxwell, JA, Lewis, TL, Accavitti-Loper, MA *et al.* (2006). Anti-Aβ single-chain antibody delivery via adeno-associated virus for treatment of Alzheimer's disease. *Neurobiol Dis* **23**: 502–511.
18. Fukuchi, K, Accavitti-Loper, MA, Kim, HD, Tahara, K, Cao, Y, Lewis, TL *et al.* (2006). Amelioration of amyloid load by anti-Aβ single-chain antibody in Alzheimer mouse model. *Biochem Biophys Res Commun* **344**: 79–86.
19. Levites, Y, Jansen, K, Smithson, LA, Dakin, R, Holloway, VM, Das, P *et al.* (2006). Intracranial adeno-associated virus-mediated delivery of anti-pan amyloid β, amyloid β40, and amyloid β42 single-chain variable fragments attenuates plaque pathology in amyloid precursor protein mice. *J Neurosci* **26**: 11923–11928.
20. Oddo, S, Caccamo, A, Shepherd, JD, Murphy, MP, Golde, TE, Kayed, R *et al.* (2003). Triple-transgenic model of Alzheimer's disease with plaques and tangles: intracellular Aβ and synaptic dysfunction. *Neuron* **39**: 409–421.
21. Billings, LM, Oddo, S, Green, KN, McGaugh, JL and LaFerla, FM (2005). Intraneuronal Aβ causes the onset of early Alzheimer's disease-related cognitive deficits in transgenic mice. *Neuron* **45**: 675–688.
22. Bobo, RH, Laske, DW, Akbasak, A, Morrison, PF, Dedrick, RL and Oldfield, EH (1994). Convection-enhanced delivery of macromolecules in the brain. *Proc Natl Acad Sci USA* **91**: 2076–2080.
23. Haidaris, CG, Malone, J, Sherrill, LA, Bliss, JM, Gaspari, AA, Insel, RA *et al.* (2001). Recombinant human antibody single chain variable fragments reactive with Candida albicans surface antigens. *J Immunol Methods* **257**: 185–202.
24. Malone, J and Sullivan, MA (1996). Analysis of antibody selection by phage display utilizing anti-phenobarbital antibodies. *J Mol Recognit* **9**: 738–745.
25. Wang, C, Wang, CM, Clark, KR and Sferra, TJ (2003). Recombinant AAV serotype 1 transduction efficiency and tropism in the murine brain. *Gene Ther* **10**: 1528–1534.
26. Sudol, KL, Mastrangelo, MA, Narrow, WC, Frazer, ME, Levites, YR, Golde, TE *et al.* (2009). Generating differentially targeted amyloid-β specific intrabodies as a passive vaccination strategy for Alzheimer's disease. *Mol Ther* **17**: 2031–2040.
27. Chen, G, Chen, KS, Knox, J, Inglis, J, Bernard, A, Martin, SJ *et al.* (2000). A learning deficit related to age and β-amyloid plaques in a mouse model of Alzheimer's disease. *Nature* **408**: 975–979.
28. Schindowski, K, Bretteville, A, Leroy, K, Bégard, S, Brion, JP, Hamdane, M *et al.* (2006). Alzheimer's disease-like tau neuropathology leads to memory deficits and loss of functional synapses in a novel mutated tau transgenic mouse without any motor deficits. *Am J Pathol* **169**: 599–616.
29. Itagaki, S, McGeer, PL, Akiyama, H, Zhu, S and Selkoe, D (1989). Relationship of microglia and astrocytes to amyloid deposits of Alzheimer disease. *J Neuroimmunol* **24**: 173–182.
30. Perlmutter, LS, Barron, E and Chui, HC (1990). Morphologic association between microglia and senile plaque amyloid in Alzheimer's disease. *Neurosci Lett* **119**: 32–36.
31. Perlmutter, LS, Scott, SA, Barrón, E and Chui, HC (1992). MHC class II-positive microglia in human brain: association with Alzheimer lesions. *J Neurosci Res* **33**: 549–558.

32. Grathwohl, SA, Kälin, RE, Bolmont, T, Prokop, S, Winkelmann, G, Kaeser, SA *et al.* (2009). Formation and maintenance of Alzheimer's disease β-amyloid plaques in the absence of microglia. *Nat Neurosci* **12**: 1361–1363.
33. Bacskai, BJ, Kajdasz, ST, Christie, RH, Carter, C, Games, D, Seubert, P *et al.* (2001). Imaging of amyloid-β deposits in brains of living mice permits direct observation of clearance of plaques with immunotherapy. *Nat Med* **7**: 369–372.
34. Koenigsknecht, J and Landreth, G (2004). Microglial phagocytosis of fibrillar β-amyloid through a β1 integrin-dependent mechanism. *J Neurosci* **24**: 9838–9846.
35. Streit, WJ, Sammons, NW, Kuhns, AJ and Sparks, DL (2004). Dystrophic microglia in the aging human brain. *Glia* **45**: 208–212.
36. Streit, WJ, Braak, H, Xue, QS and Bechmann, I (2009). Dystrophic (senescent) rather than activated microglial cells are associated with tau pathology and likely precede neurodegeneration in Alzheimer's disease. *Acta Neuropathol* **118**: 475–485.
37. Lambert, MP, Velasco, PT, Chang, L, Viola, KL, Fernandez, S, Lacor, PN *et al.* (2007). Monoclonal antibodies that target pathological assemblies of Aβ. *J Neurochem* **100**: 23–35.
38. Mastrangelo, MA and Bowers, WJ (2008). Detailed immunohistochemical characterization of temporal and spatial progression of Alzheimer's disease-related pathologies in male triple-transgenic mice. *BMC Neurosci* **9**: 81.